d-OptCom: Dynamic Multi-level and Multi-objective Metabolic Modeling of Microbial Communities

Ali R. Zomorrodi,[†] Mohammad Mazharul Islam,[†] and Costas D. Maranas*

Department of Chemical Engineering, Pennsylvania State University, University Park, Pennsylvania 16802, United States

Ⓢ Supporting Information

ABSTRACT: Most microbial communities change with time in response to changes and/or perturbations in environmental conditions. Temporal variations in interspecies metabolic interactions within these communities can significantly affect their structure and function. Here, we introduce d-OptCom, an extension of the OptCom procedure, for the dynamic metabolic modeling of microbial communities. It enables capturing the temporal dynamics of biomass concentration of the community members and extracellular concentration of the shared metabolites, while integrating species- and community-level fitness functions. The applicability of d-OptCom was demonstrated by modeling the dynamic co-growth of auxotrophic mutant pairs of *E. coli* and by computationally assessing the dynamics and composition of a uranium-reducing community comprised of *Geobacter sulfurreducens*, *Rhodoferax ferrireducens*, and *Shewanella oneidensis*. d-OptCom was also employed to examine the impact of lactate vs acetate addition on the relative abundance of uranium-reducing species. These studies highlight the importance of simultaneously accounting for both species- and community-level fitness functions when modeling microbial communities, and demonstrate that the incorporation of uptake kinetic information can substantially improve the prediction of interspecies flux trafficking. Overall, this study paves the way for the dynamic multi-level and multi-objective analysis of microbial ecosystems.

KEYWORDS: microbial communities, dynamic modeling, flux balance analysis, multi-objective optimization
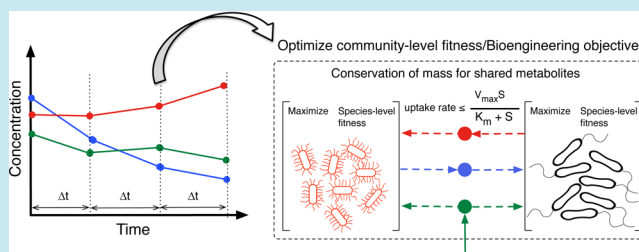
Microbial communities are involved in a wide range of biological and biotechnological processes. For example, they are responsible for driving biogeochemical cycles of carbon and nitrogen[1] and play fundamental roles in human health and disease.[2–5] The unique metabolic capabilities of these communities have been harnessed for biofuel production,[6,7] biodegradation of alkanes, and natural attenuation of pollutants,[8–11] dissimilatory metal reduction from subsurface environments,[12–14] biological wastewater treatment,[15,16] and more.[17] Members of a microbial community can interact by unidirectional or bidirectional exchange of metabolites or charged compounds giving rise to mutualism, synergism, commensalism, parasitism, or competition among community members.[18–21] Microbial communities are known to exhibit dynamic shifts in their metabolism as well as in their interspecies interactions in response to perturbations in environmental condition in order to support co-growth, survival, and stability[22,23].[24] A well-known example is the day–night or seasonal variations.[25,26] The interspecies interactions and their temporal changes play pivotal roles in shaping the community composition, structure, and function;[27] however, the nature of these interactions and their dynamic variations are not well understood yet.

With the ever-increasing availability of reconstructed metabolic models of microorganisms a number of methods based on the constraint-based analysis have been developed recently to study the steady-state behavior of simple microbial consortia.[22,27–33] The pioneering effort was modeling a two-member mutualistic microbial community consisting of a sulfate-reducing bacteria and a methanogen using a multi-species compartmentalized stoichiometric metabolic model.[27] A similar approach was employed for the metabolic modeling of a syntrophic association between *Clostridium butyricum* and *Methanosarcina mazei*.[28] In another effort, a workflow was presented by Lewis et al.[29] to model human metabolism within and between different types of cells. On another front, Wintermute and Silver[22] proposed a procedure to identify the mutualistic relationships in pairs of auxotrophic *E. coli* mutants, where each pair was modeled using an extended form of the minimization of metabolic adjustment (MOMA) hypothesis.[34] Nagarajan et al.[31] proposed a multi-omics modeling workflow, combining genomic, transcriptomic, and physiological data with genome-scale models to assess interspecies electron transfer in a syntrophic microbial community comprising of two *Geobacter* species. By assessing the entire spectrum of feasible interactions between the partners using phenotypic phase plane analysis,[32] they identified distinct optimal and suboptimal phases of
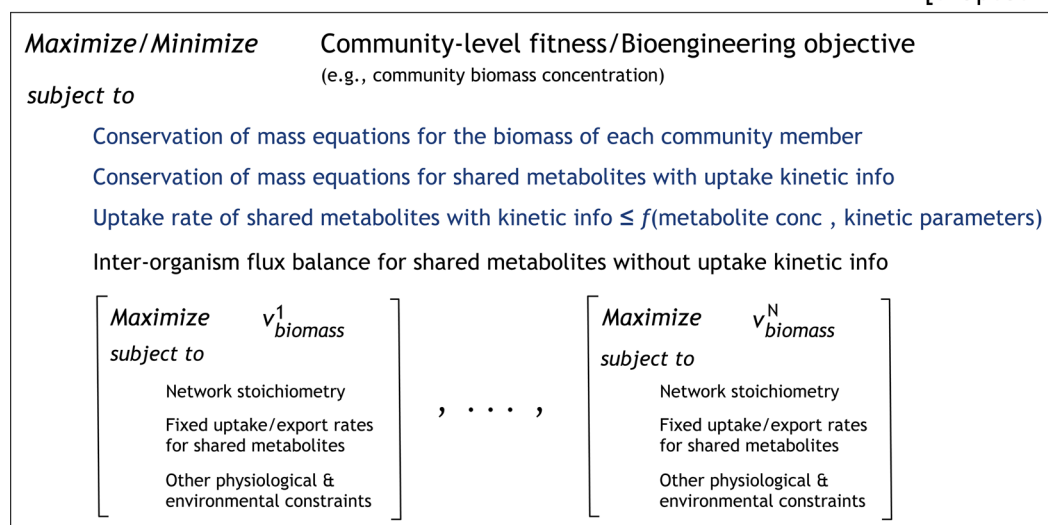
Figure 1. Optimization structure of d-OptCom. Dynamic equations representing the conservation of mass for the biomass of each species and each shared metabolite with available uptake kinetics are added as new constraints to the outer problem. The upper bounds on uptake rates are determined by using uptake kinetic expressions.

interspecies electron transfer. A number of other approaches that are not based on flux balance analysis (FBA) have been also attempted for modeling of microbial communities including elementary mode analysis, evolutionary game theory, nonlinear dynamics, and stochastic processes.[35−41]

Given that the microbial metabolism and metabolic interactions in microbial communities are of an intrinsic dynamic nature as noted earlier, a dynamic modeling framework is an absolute necessity to explore the experimentally testable and/or unverifiable hypotheses. Despite the availability of dynamic modeling frameworks for single species,[42,43] the development of community-level dynamic models is a challenging task due to the increased complexity and incomplete knowledge about the dynamics of interspecies interactions over a changing environment. There have been a number of recent efforts aimed to address this challenge,[12,30,33,44−47] most of which are based on the extension of the dynamic flux balance analysis (dFBA) for single species.[42] The first attempt in this direction was a computational framework called the Dynamic Multi-species Metabolic Modeling (DMMM) proposed by Zhuang et al.[12] This procedure is based on an extension of the dFBA[42] for individual species and was used to model the competition between *Rhodoferax ferrireducens* and *Geobacter sulfurreducens* in an anoxic subsurface environment under both naturally occurring and manually stimulated conditions. The same procedure was employed for modeling another community comprised of *Clostridium acetobutylicum* and *Clostridium cellulolyticum*.[45] Hanly and Henson[46,47] also used a similar procedure based on dFBA to model dynamics of microbial co-cultures of *E. coli* and *S. cerevisiae*[46] as well as respiratory-deficient *Saccharomyces cerevisiae* and wild-type *Scheffersomyces stipitis* strains.[47] Zhuang et al.[44] later proposed an extension of their earlier DMMM[12] approach to devise a long-term practical bioremediation strategy for uranium reduction. In a more recent study, Minty et al.[23] developed another framework where the dynamic co-growth of two species is simulated by solving a system of ordinary differential equations (ODEs) representing mass balances in a batch culture and hierarchical

clustering techniques are used to reveal feasible region of substrate partition between competing community members. This procedure was employed for the characterization of a synthetic fungal−bacterial consortium for the efficient biosynthesis of valuable products (e.g., isobutanol) from lignocellulosic feedstock.

Despite these efforts, all the methods described so far (except for the studies of Zhuang et al.[44] and Minty et al.[23]) are based on optimization problems with a single objective function. As such, a comprehensive dynamic modeling framework capable of simultaneously accommodating multiple species- and community-level fitness criteria is still lacking. To capture the multi-level nature of decision making in microbial communities, we previously introduced OptCom[48] that uses a multi-level and multi-objective optimization formulation capable of capturing both species- and community-level fitness criteria. Here, we introduce d-OptCom (dynamic OptCom) for the multi-objective dynamic analysis of microbial communities. d-OptCom incorporates the dynamic mass balance equations and substrate uptake kinetics in its modeling framework and enables the direct assessment of the shared metabolites and biomass concentrations in a given community. This procedure was used first to model dynamics of the co-growth of *E. coli* auxotrophic mutant pairs. It was then employed to elucidate the impact of the addition of a new member to a uranium-reducing microbial community on its growth, dynamics, and composition, as well as to assess the efficacy of lactate and acetate injection to enhance uranium reduction. These analyses show the importance of integrating species- and community-level fitness functions and reaffirm the impact of incorporating kinetic information in improving the prediction of interspecies fluxes.

■ METHODS

The original OptCom procedure is a multi-level and multi-objective optimization framework that postulates a separate biomass maximization problem for each community member as inner problems.[48] Interspecies interactions are modeled by using constraints in the outer problem imposing a flux balance
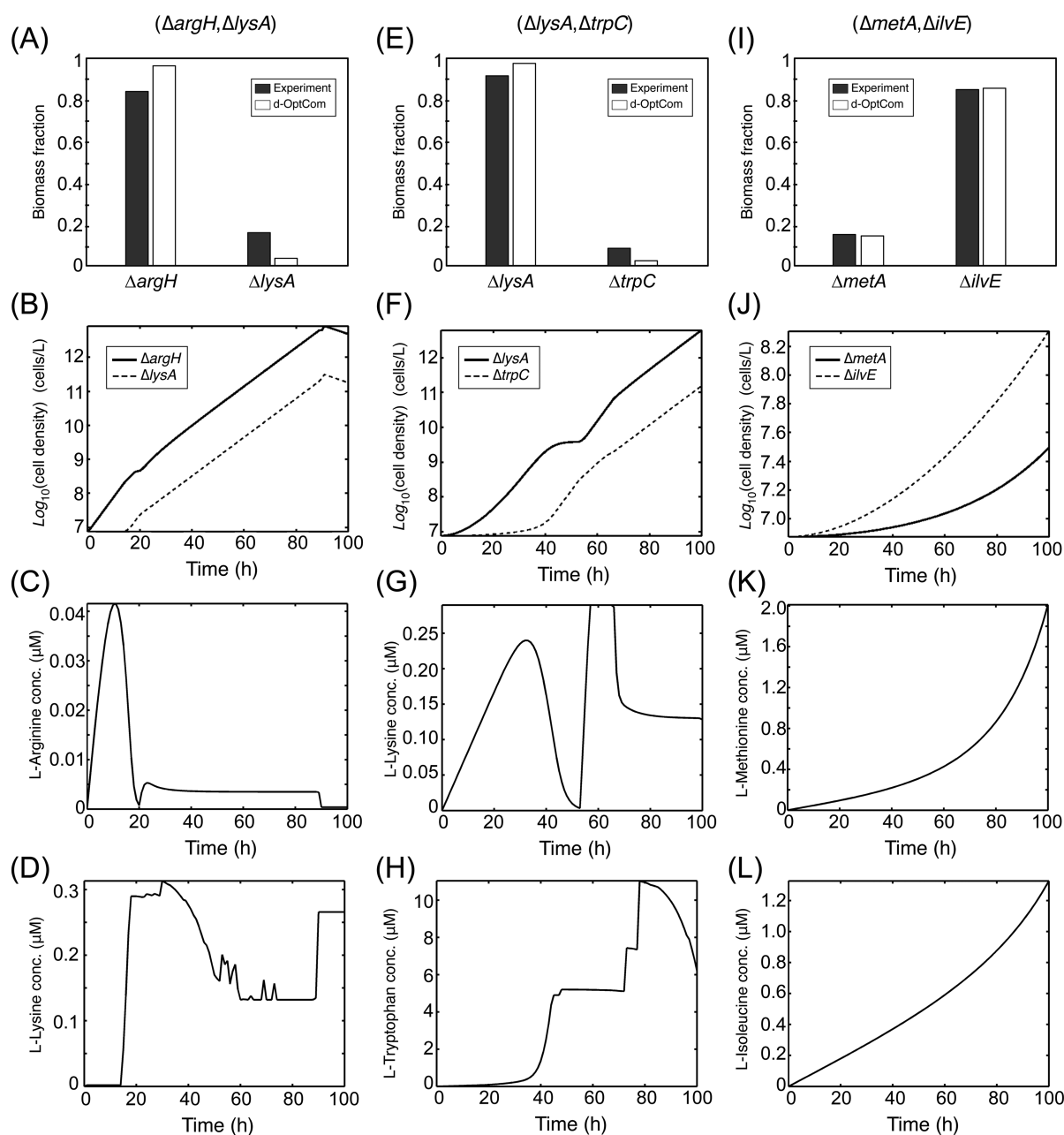
Figure 2. Modeling the co-growth of auxotrophic *E. coli* mutant pairs using d-OptCom. A, E, and I compare the predicted biomass fraction of each species after four days (96 h) with experimental measurements.[22] B, F, and J indicate the predicted cell density of each community member using d-OptCom, and C, D, G, H, K, and L show the predicted extracellular concentration of the shared amino acids. The biomass fraction of each species in A, E, and I was computed by dividing the species cell density (cells/L) by the sum of cell densities of both community members.

in the extracellular environment for each shared metabolite. Inner problems are integrated and linked with each other by using inter-organism flow constraints so as to optimize an outer-level objective function. The objective function of the outer problem represents a community-level fitness criterion, or surrogates a desired (community) engineering objective. Descriptive OptCom is a modified mode of OptCom, which enables quantification of the deviation of individual species from their optimal growth phenotype consistent with experimental observations. This is achieved by incorporating any available experimental data about the entire community or individual species in the optimization problem using new constraints in the outer problem, or inner problems of the respective species, respectively. Deviation of each species from

its optimal behavior is measured using a metric called "optimality level", which can take a value of less than, equal, or greater than one representing, suboptimal, optimal, or superoptimal behavior of the community members.[48] More details about OptCom and Descriptive OptCom as well as an improved solution procedure using the KKT conditiona is given in Supporting Information.

Dynamic Modeling of Microbial Communities Using d-OptCom. The OptCom procedure was extended to capture dynamic changes in microbial communities. To this end, new time-dependent constraints representing the conservation of mass for the biomass of each species and shared metabolites with available uptake kinetics are added to the outer problem (see Figure 1). The upper bound on uptake rate of each shared

metabolite is determined by using the uptake kinetic expressions incorporated as additional constraints in the outer problem. The inter-organism flow constraint (from the original OptCom procedure) is used instead of conservation of mass equations for each shared metabolite without any uptake kinetics. The uptake/export rates of shared metabolites are determined by the outer problem; however, they act as parameters for inner problems of the respective community members. This multi-level optimization problem can be recast as a nonlinear problem or a mixed-integer nonlinear problem by using the strong duality or KKT conditions for inner problems, respectively. In both cases the problem is, in general, nonconvex due to the presence of uptake kinetic expressions and conservation of mass equations. Therefore, we used the global optimization solver BARON[49] accessible via GAMS and/or GlobalSearch function in MATLAB (MathWorks Inc.) to solve the case studies presented in this paper to global optimality. Details of the d-OptCom procedure and its solution procedure are given in Supporting Information.

d-OptCom enables not only capturing the dynamic behavior of microbial communities but also incorporation of the biomass and shared metabolite concentrations in the modeling framework. For example, it is possible to maximize the total biomass concentration of the community instead of maximizing the total biomass flux of the community (i.e., sum of the biomass fluxes of community members) as used in the original OptCom procedure. Alternatively, one can maximize (minimize) the concentration of a desired (undesired) shared metabolite or minimize deviation from a target time-dependent concentration pattern as the engineering objective. Furthermore, this extends the concept of Descriptive OptCom[48] to a dynamic context (i.e., Descriptive d-OptCom) where constraints on actual extracellular concentrations (e.g., the biomass composition of the community) can be added to the outer (or inner) problem(s) in order to determine dynamic changes in optimality level of each community member.

Dynamic Modeling in the Absence of Uptake Kinetics. In the absence of uptake kinetics for all the shared metabolites, instead of using the ON/OFF method[12] (allowing the unlimited uptake of the shared metabolites by each community member), regular OptCom can be used in a dynamic fashion by successively applying it in consecutive time intervals in order to identify how the inter-organism metabolite traffic flows should be apportioned among the community members to satisfy the community-level fitness (or engineering objective). Similarly, Descriptive OptCom can be used within each time interval to identify the optimality levels of community members consistent with available experimental observations (see Supporting Information for an example).

RESULTS AND DISCUSSION

Co-growth of Auxotrophic *E. coli* Mutant Pairs. We used d-OptCom to model and analyze the dynamics of a synthetic mutualistic relationship between pairs of auxotrophic *E. coli* mutants. Wintermute and Silver[22] previously examined the co-growth of several combinations of 46 mutant strains, where the deletion(s) in each strain blocks the biosynthesis of a biomass precursor such as amino acids, nucleotides, or cofactors. Each strain is able to grow in the rich (LB) medium but not in the minimal (M9) medium. Certain pairs of dissimilar mutant strains were observed to be capable of complementing one another's growth in the minimal medium through cross-feeding the essential metabolites.[22] These mutant

pairs show a higher growth in the co-culture compared to individual growth in supplemented minimal medium. Wintermute and Silver[22] measured the community growth each day over four days and biomass fraction of each species after four days.

Here, we examined whether d-OptCom is capable of recapitulating the co-growth of cooperating partners. To this end, we selected three such mutant pairs comprised of four genes involved in the production of different amino acids with available uptake kinetics. These pairs include ($\Delta argH$, $\Delta lysA$), ($\Delta lysA$, $\Delta trpC$), and ($\Delta metA$, $\Delta ilvE$), where the deletion of *argH*, *lysA*, *trpC*, *metA*, and *ilvE* block the production of L-arginine, L-lysine, L-tryptophan, L-methionine, and L-isoleucine, respectively. We assumed that the blocked amino acids are the primary metabolites being shared between the two partners; however, it is worth noting that some auxotrophic mutants could rescue one another by sharing not necessarily the missing amino acid but instead a precursor thereof. For example, certain tryptophan deficient mutants can be rescued by sharing indole instead of tryptophan.[22] The *iAF1260* model of *E. coli*[50] was used for this study, and gene knockouts were simulated by setting the flux of corresponding reactions in the model to zero. Maximization of the total community biomass concentration (cells/L) was chosen as the outer (community-level) objective function, and each species was assumed to maximize its biomass flux in the inner problems. The initial concentration of the shared amino acids was set to zero, and the simulation horizon was 100 h (details of simulation parameters are given in Supporting Information). The predicted biomass fraction of each species after four days as well as the dynamic changes in cell densities and shared amino acid concentrations for each mutant pair are represented in Figure 2. As shown in this figure d-OptCom can successfully predict the co-growth of all three mutant pairs, and in addition, the predicted biomass fraction of each partner is in good agreement with experimental measurements for all three mutant pairs (see Figure 2A, E, and I). For example, d-OptCom predicts that the co-culture of $\Delta metA$ and $\Delta ilvE$ is composed of 14.40% $\Delta metA$ and 85.60% $\Delta ilvE$ after four days (96 h), which is very close to 15.08% and 84.02% measured experimentally.[22] The higher biomass fraction of $\Delta ilvE$ was correctly predicted by d-OptCom, as it incorporates the substrate uptake kinetics. For example, V_{max} and K_m for L-isoleucine uptake are 0.0346 mmol/gDW·h and 1.22×10^{-3} mM, whereas those for L-methionine are 0.0140 mmol/gDW·h and 2.3×10^{-3} mM. In the absence of any uptake kinetics (e.g., using regular OptCom), approximately equal biomass fractions are predicted for both partners as long as the stoichiometric coefficients of the shared amino acids in the biomass reaction are not significantly different. As shown in Figure 2, the selected mutant pairs expand their own pool of required amino acids by aiding the growth of their conjugate partners. This cooperative behavior was captured by d-OptCom as it simultaneously takes into account species and community-level fitness functions enabling it to identify the impact of interspecies interactions on the shared metabolite and biomass concentrations. In contrast, simulation of the same mutant pairs with DMMM procedure[12] did not predict any co-growth. This is because in the absence of a community-level fitness function participating species do not have any incentive to cooperate, even though the initial concentration of the essential amino acids was zero. This study underlines the usefulness of a community-level fitness function in cooperative microbial communities.

Dynamic Analysis of Subsurface Uranium-reducing Communities. *Geobacter sulfurreducens* and *Rhodoferax ferrireducens* are known to be capable of dissimilatory metal reduction in anoxic subsurface environments[13] reducing Fe(III) to Fe(II) while oxidizing acetate. *G. sulfurreducens* can also reduce U(VI) to U(IV),[51,52] making it a suitable candidate for bioremediation applications in uranium-contaminated groundwater.[53,54] Growth of *G. sulfurreducens* and *R. ferrireducens* rely on the acetate produced by other microorganisms present in the community (such as *Clostridia* and *δ-proteobacteria*[55]) as the carbon source. In addition to acetate, these two microorganisms compete for ammonium and Fe(III) in the subsurface communities of Rifle, CO. Genome-scale metabolic models for these two microorganisms were reconstructed before.[56−58] These models were used by Zhuang et al.[12] for the metabolic modeling of this community using the DMMM framework and to design long-term uranium bioremediation strategies.[44]

Here, we examined the impact of the addition of an acetate-producing member to the *G. sulfurreducens*–*R. ferrireducens* community by using the d-OptCom procedure. We chose *Shewanella oneidensis* as it is a known acetate producer[59−61] with a reconstructed genome-scale metabolic model.[59] In addition, *S. oneidensis* can reduce U(VI) to U(IV),[52] coupling this reduction with the oxidation of lactate. The combined uranium reduction capability of *S. oneidensis* and *G. sulfurreducens* may thus promise a more effective bioremediation strategy. The metabolic interactions of the three-member community composed of *S. oneidensis*, *G. sulfurreducens*, and *R. ferrireducens* are shown in Figure 3. We assumed that lactate is
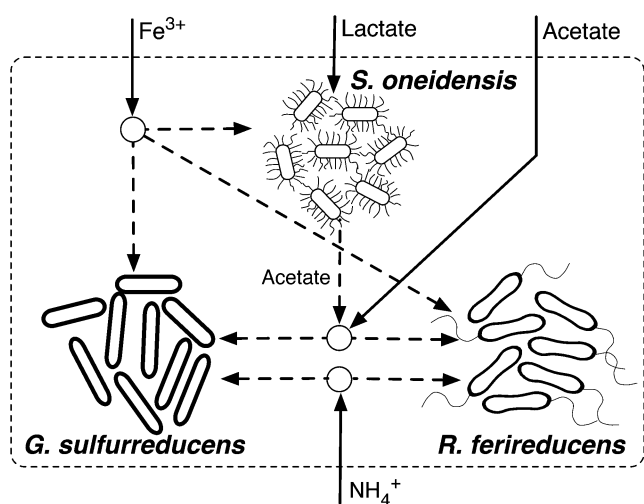
Figure 3. Pictorial representation of the metabolic interactions in anoxic subsurface uranium-reducing communities in the presence of *S. oneidensis*. Acetate is supplied to *G. sulfurreducens* and *R. ferrireducens* by *S. oneidensis* as well as by other microorganisms present in the community.

the sole available carbon source for *S. oneidensis* in the community. Neither *G. sulfurreducens* nor *R. ferrireducens* are capable of metabolizing lactate and thus rely on the acetate produced by *S. oneidensis* and other community members. Notably, while *S. oneidensis* supplies acetate to *G. sulfurreducens* and *R. ferrireducens*, it also competes with them for Fe(III). Maximization of the biomass 'flux' (h^{-1}) was used in the inner problems of d-OptCom to capture the species-level driving forces and maximization of biomass 'concentration' of the entire community (cells/L) was chosen as the community-level

objective function. All simulations were performed under the ammonium excess condition (i.e., $[NH_4] = 400\ \mu M^{12}$). Ammonium, acetate, and Fe(III) uptake kinetic parameters for *G. sulfurreducens* and *R. ferrireducens* as well as environmental parameters were all obtained from Zhuang et al.[12] The lactate uptake kinetics for *S. oneidensis* was estimated from the growth kinetics on this carbon source[62] by using FBA (see Supporting Information for details). Similar to *R. ferrireducens*, the Fe(III) uptake kinetics of *S. oneidensis* was assumed to be the same as *G. sulfurreducens*.[12] The lactate concentration in the medium was assumed to be 5 mM.[63−65] Furthermore, the subsurface environment in the Rifle site was modeled as a chemostat similarly to the previous studies.[12] All simulation parameters are provided in the Supporting Information.

We assessed how the biomass composition of this three-member community changes with time as a function of the combined positive and negative interspecies interactions. Dynamic simulations using d-OptCom show that in the long run *S. oneidensis* dominates the co-culture almost completely (see Figure 4). This can be attributed to the higher growth yield and better uptake efficiency of *S. oneidensis* when growing on lactate compared to those of *G. sulfurreducens* and *R. ferrireducens* when growing on acetate. For example, V_{max} for the lactate uptake by *S. oneidensis* was estimated to be 75 mmol/gDW·h, which is more than 5 and 53 times greater than the V_{max} of *G. sulfurreducens* (13.3 mmol/gDW·h) and *R. ferrireducens* (1.71 mmol/gDW·h) for acetate uptake, respectively. In addition, FBA simulations show that with the same Fe(III) uptake rate, the growth yield of *S. oneidensis* on lactate (0.68 gDW/mmol per 100 mmol of lactate uptake) is almost twice that for *G. sulfurreducens* (0. 33 gDW/mmol per 100 mmol of acetate uptake), and more than six times greater than the growth yield of *R. ferrireducens* on acetate (0.11 gDW/mmol per 100 mmol of acetate uptake).

Comparison of OptCom and d-OptCom Predictions. Simulation of the three-member community using regular OptCom was performed with maximization of the biomass flux of the entire community as the outer objective function. This analysis revealed that the observed long-term behavior of the community cannot be captured by the regular OptCom procedure. For example, regular OptCom predicts that with the estimated lactate and acetate community uptake rates under natural subsurface conditions[12,66] (see Supporting Information for details), *S. oneidensis* constitutes only 35% of the total community biomass (assuming that the ratio of biomass fluxes is proportional to the respective biomass fractions).

This inconsistency is because regular OptCom simulates only a snapshot of the dynamic behavior close to initial condition. In addition, in the absence of any kinetic information, it freely apportions the shared resources to the community members so as to optimize the community-level objective function. Another contributing factor to this inconsistency is the difference in the way component balances are handled by OptCom and d-OptCom for shared metabolites. While the former simply balances the uptake and export fluxes of the shared metabolites, the latter takes into account both fluxes and concentrations when imposing mass balances. For example, if *S. oneidensis* produces 10 mmol/gDW·h of acetate, regular OptCom predicts that the same amount is directly available to *G. sulfurreducens* and *R. ferrireducens*, whereas according to the conservation of mass equations incorporated in d-OptCom, the uptake rate of acetate by these two species is determined by both uptake kinetics and cell density of *S. oneidensis* in the community.
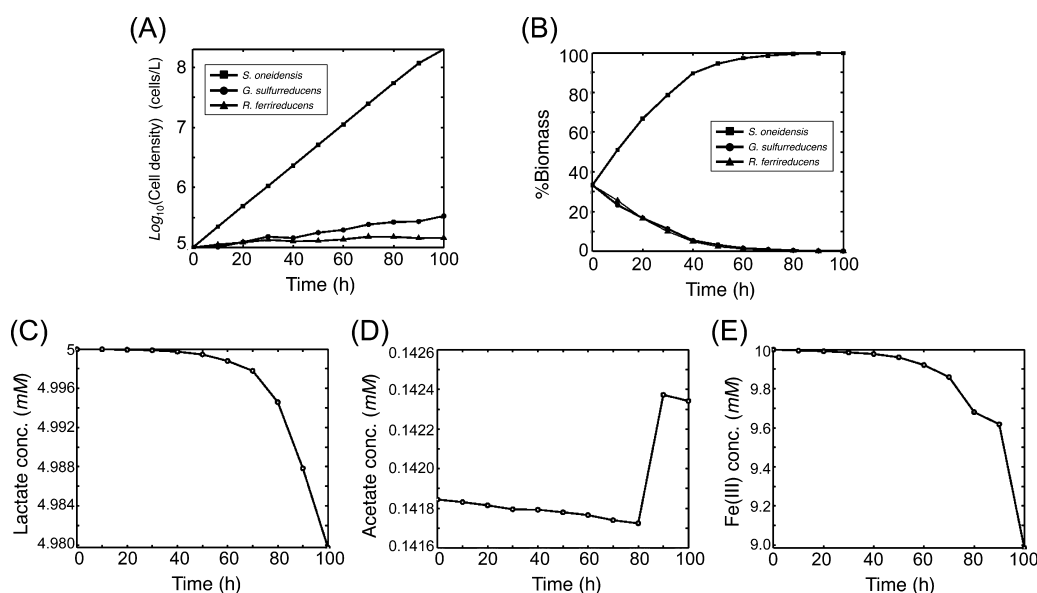
Figure 4. Dynamic behavior of the three-member community composed of *S. oneidensis*, *G. sulfurreducens*, and *R. ferrireducens* as predicted by d-OptCom. (A) Cell density of each community member (cells/L) on a logarithmic scale. (B) Biomass fraction of each species computed using the cell densities, (C) Lactate concentration, (D) acetate concentration, and (E) Fe(III) concentration. The simulations were performed for a lactate concentration of 5 mM and acetate turnover rate of 0.2 μM/h, while modeling the Rifle site as a chemostat. The points on the curves represent the simulation results and the connections between the discrete simulation points are just for the ease of representation.
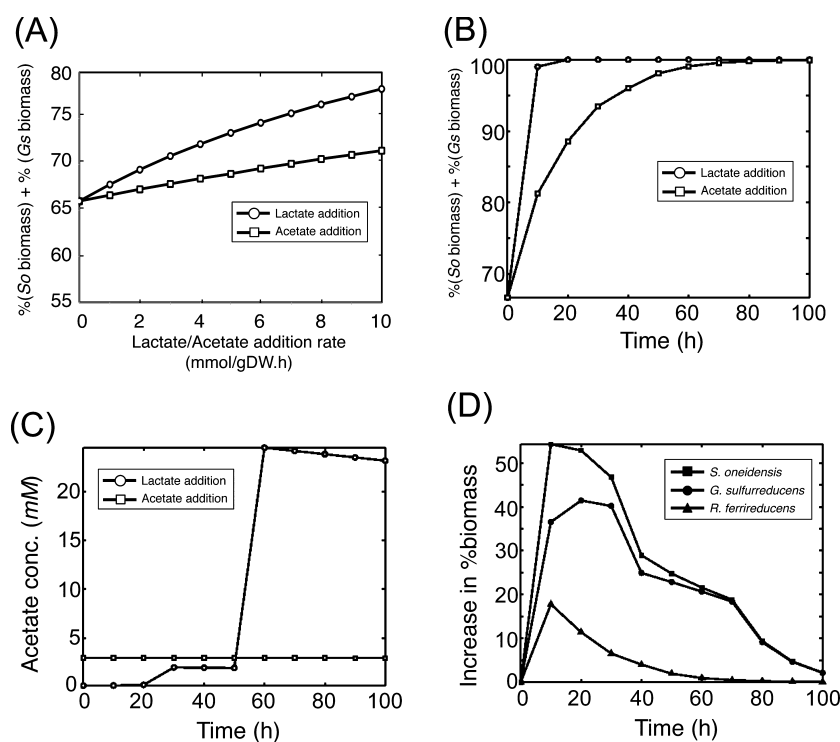
Figure 5. Comparison of the effect of lactate and acetate injection on the combined biomass fractions of the U(VI)-reducing species (*S. oneidensis* and *G. sulfurreducens*) So, Gs, and Rf stand for *S. oneidensis*, *G. sulfurreducens*, and *R. ferrireducens*, respectively. (A) using regular OptCom (where biomass fractions are computed based on the ratio of biomass fluxes) and (B) using dynamic simulations with d-OptCom (where biomass fractions are computed using the cell densities). (C) Concentration of the acetate in the medium (using d-OptCom), and (D) absolute value of the difference between the predicted biomass fraction of each species under the lactate and acetate injection condition (using d-OptCom). The biomass fraction of *S. oneidensis* is higher under the lactate injection condition, whereas that for *G. sulfurreducens* and *R. ferrireducens* is higher under the acetate injection. Lactate and acetate addition for d-OptCom simulations were modeled by using a lactate concentration of 105 mM, and an acetate turnover rate of 4.2 μM/h,[12] respectively. The points on curves represent simulation results and the connections between discrete simulation points are just for the ease of representation.

Therefore, the rate of change in the acetate concentration due to 10 mmol/gDW·h of acetate production by *S. oneidensis* will

be only 6.4×10^{-7} (mmol/h) for a cell density of 10^5 (cells/L) and 6.4×10^{-4} (mmol/h) for a cell density of 10^8 (cells/L) of *S.*
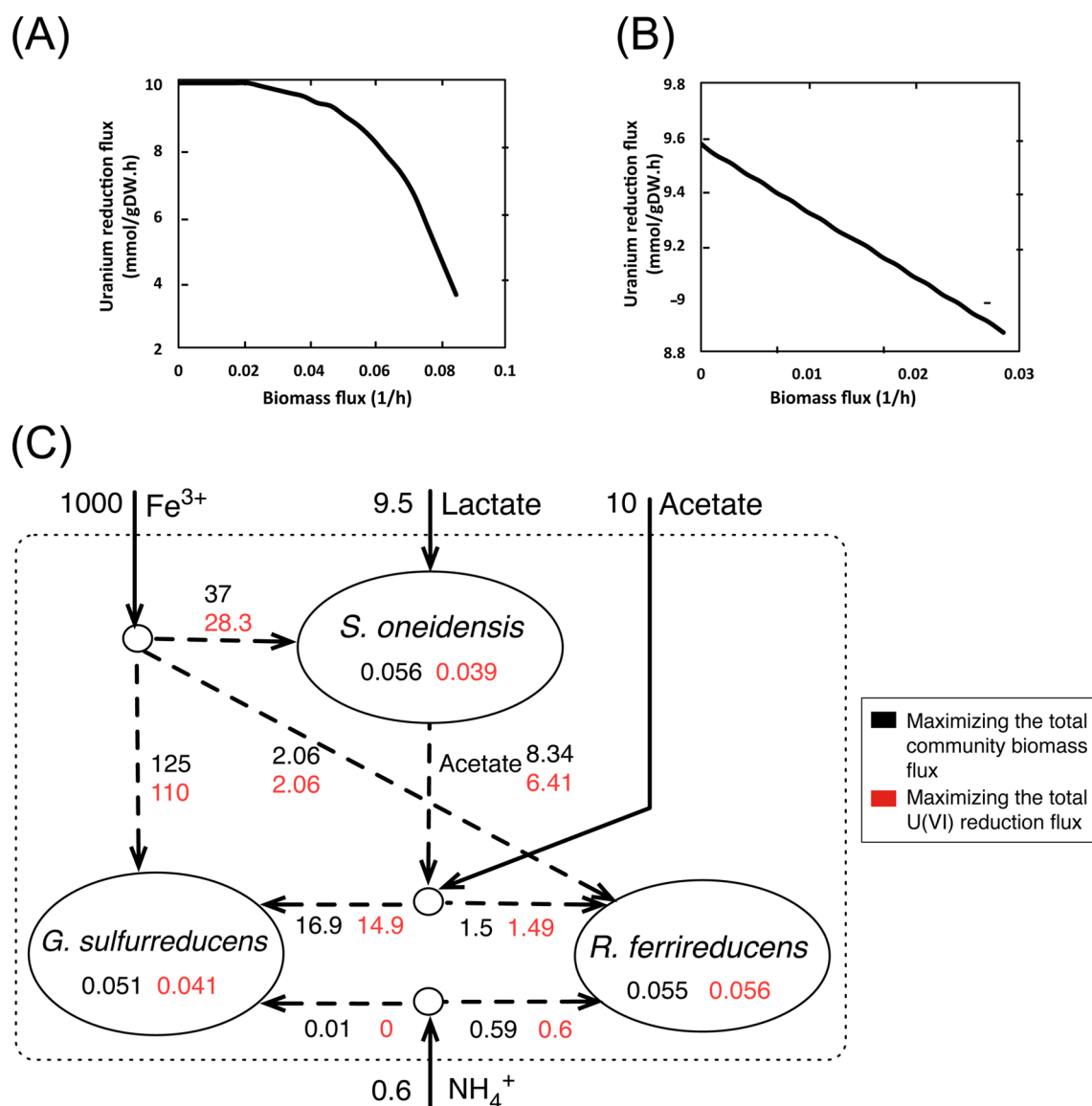
Figure 6. Uranium reduction flux in (A) *S. oneidensis* and (B) *G. sulfurreducens* as a function of biomass flux. (C) Comparison of the predicted biomass and interspecies exchange fluxes using regular OptCom, when maximizing the total community biomass flux (sum of the biomass fluxes of all three species) and maximizing the sum of the uranium reduction fluxes in *G. sulfurreducens* and *S. oneidensis*.

oneidensis (cell mass of *S. oneidensis* was set at 6.4×10^{-7} following previous reports[12]). As such, the shared metabolite distribution scenarios predicted by regular OptCom may not always be consistent with d-OptCom predictions. For example, according to the OptCom simulations, *G. sulfurreducens* can take up 16.9 mmol/gDW·h of acetate while maximizing the entire community biomass flux. In contrast, d-OptCom results indicate that this rate cannot exceed 7.45 mmol/gDW·h over the course of the dynamic simulations. This implies that the flux distribution of the shared metabolites is more restricted in d-OptCom, compared to regular OptCom as the uptake efficiencies (determined by uptake kinetics), cell densities and extra-cellular concentrations of the shared metabolites can significantly limit the uptake rates of the shared resources by different community members.

Analysis of the Impact of Lactate vs Acetate Amendment on the Biomass Composition. Acetate injection in Rifle site has been reported to lead to an increase in the *G. sulfurreducens* fraction and as a result an increase in uranium reduction.[12,13]

We computationally assessed using OptCom and d-OptCom, the impact of an alternative strategy, which is the injection of lactate, the preferred carbon source for *S. oneidensis*.

OptCom Predictions. Different lactate and acetate uptake conditions were examined using regular OptCom, while keeping Fe(III) and ammonium uptake rates constant (see Supporting Information for details). The rate of addition of lactate (or acetate) was initialized at zero and increased by 1 mmol/gDW·h at each time interval. As shown in Figure 5A, addition of lactate leads to a higher combined biomass fraction of the U(VI)-reducing species (i.e., *S. oneidensis* and *G. sulfurreducens*) compared to the acetate addition (assuming that the ratio of biomass fluxes is proportional to that of biomass concentration). For example, for a lactate injection rate of 5 mmol/gDW.h (i.e., the total available lactate of 5 + 9.5 = 14.5 mmol/gDW·h), *S. oneidensis* and *G. sulfurreducens* form 73.4% of the total community biomass (according to biomass fluxes) whereas for the same acetate uptake rate this percentage is reduced to 69.0%. This is because according to OptCom

predictions, addition of lactate not only increases the growth of *S. oneidensis*, but it can also increase the acetate production by *S. oneidensis*, thereby enhancing the growth of both *G. sulfurreducens* and *R. ferrireducens*. For example, according to the simulation results, the production of acetate by *S. oneidensis* with a lactate injection rate of 5 mmol/gDW·h is 12.7 mmol/gDW·h providing a total of (12.7 + 10 =) 22.7 mmol/gDW·h of acetate, to the community members. On the other hand, addition of 5 mmol/gDW·h acetate (i.e., total available acetate of 5 + 10 = 15 mmol/gDW·h) only supports the growth of *G. sulfurreducens* and *R. ferrireducens* but not that of *S. oneidensis*, thus decreasing the total fraction of U(VI) reducers in the community.

d-OptCom Predictions. Consistent with the regular OptCom, dynamic simulations with d-OptCom show that addition of lactate leads to a higher combined biomass fraction of *S. oneidensis* and *G. sulfurreducens* (see Figure 5B). In addition, *S. oneidensis* is predicted to dominate the community again in the long run, irrespective of whether lactate or acetate is added. In contrast to OptCom, d-OptCom, however, reveals that the increase in the acetate concentration in the medium after the injection of lactate is very small, even though its concentration increases sharply after the dominance of the co-culture by *S. oneidensis* (see Figure 5C) as the fraction of acetate consuming species (i.e., *G. sulfurreducens* and *R. ferrireducens*) decrease dramatically. This suggests that the increased availability of acetate in the medium is less likely to be the only contributing factor to the higher combined biomass fractions of the U(VI)-reducing species after the lactate injection. This could instead be due to the superior lactate uptake kinetics and growth yield of *S. oneidensis* compared to those of *G. sulfurreducens* and *R. ferrireducens* for acetate, as noted earlier. This hypothesis was confirmed by plotting the predicted increase in the biomass fractions of each of these species under the lactate and acetate amendment condition (Figure 5D). Figure 5D shows that the increase in the biomass fraction of *S. oneidensis* due to the lactate addition is always higher than (or equal to) the increase in the *G. sulfurreducens* and *R. ferrireducens* fractions due to acetate injection. In other words, even though the acetate amendment has a high impact on the growth of *G. sulfurreducens* and *R. ferrireducens*, its contribution to the combined biomass fractions of U(VI)-reducing species is smaller compared to the significant increase in the fraction of *S. oneidensis* due to the lactate injection. These results suggest that the addition of lactate to this community may be a more effective bioremediation strategy to enhance U(VI) reduction compared to the addition of acetate. Moreover, given that *S. oneidensis* dominates the community in the long run, addition of this microorganism to the Rifle site may also be considered as an alternative to the acetate or lactate amendment.

Modeling the Uranium Reduction Capability of the Community. The metabolic models of *G. sulfurreducens* and *S. oneidensis* were expanded to directly capture the U(VI) reduction capability using an electron capacitance model proposed by Zhao et al.[67,68] It is unknown whether U(VI) reduction is coupled with growth in *G. sulfurreducens* and *S. oneidensis*.[69–71] Plotting the flux of uranium reduction as a function of the cell growth shows a rather competitive behavior of uranium reduction flux and biomass flux for both *G. sulfurreducens* and *S. oneidensis* (see Figure 6A and B). This is because a portion of the available carbon source (lactate for *S. oneidensis*, and acetate for *G. sulfurreducens*), serving as the sole

electron donor in the system, has to be used for the extracellular uranium reduction instead of growth.

Here, we sought to maximize the Uranium reduction capability of the community (i.e., sum of the fluxes of the uranium reduction reactions in *G. sulfurreducens* and *S. oneidensis*) using regular OptCom, in order to identify how interspecies flux distribution is affected compared to maximization of the entire community biomass flux. The biomass of each species was constrained to be at least 10% of their maximum. The analysis shows that maximization of the uranium reduction flux results in a decrease in the biomass flux of the uranium-reducing species, namely *G. sulfurreducens* and *S. oneidensis* (see Figure 6C): The biomass flux of *S. oneidensis* and *G. sulfurreducens* decrease by 30% and 20%, respectively, while the biomass of *R. ferrireducens* shows an increase by only 2%. In addition, the uptake rate of Fe(III) by *G. sulfurreducens* and *S. oneidensis* decreases by 12% and 23.5%, respectively, while that for *R. ferrireducens* remains unaffected. More importantly, the acetate production by *S. oneidensis* decreases by 23% when maximizing the uranium reduction capability of the community. All these observations can be explained by the electron capacitance model,[67,68] as maximization of the uranium reduction flux requires rerouting a significant portion of the carbon flow from biomass formation, byproduct production (i.e., acetate production by *S. oneidensis*) and Fe(III) reduction toward uranium reduction. This implies that the increased availability of the carbon source for the uranium-reducing species (i.e., lactate for *S. oneidensis* and acetate for *G. sulfurreducens*) as well as that for Fe(III) can improve the uranium reduction. Even though lactate addition was shown here to lead to a higher increase in the combined biomass fraction of the uranium-reducing species, further analyses using d-OptCom is needed to assess the impact of lactate and acetate addition on the actual uranium concentration in the environment.

■ SUMMARY AND CONCLUSIONS

In this study, we introduced d-OptCom, an extended version of the OptCom procedure[48] for the dynamic, multi-level, and multi-objective metabolic modeling of microbial communities. d-OptCom incorporates substrate uptake kinetics, whenever available, into its modeling framework and accommodates the time-dependent changes in biomass and extracellular concentrations of the shared resources by using conservation of mass equations and couples them with conventional flux balance analysis methods. Application of d-OptCom to model the cross feeding of auxotrophic *E. coli* mutant pairs demonstrated the need for simultaneously accounting for species- and community-level fitness functions in a unified framework. The dynamic analysis of uranium-reducing communities with an additional member showed that the incorporation of kinetic information can significantly sharpen the inference of inter-organism metabolite trafficking due to the concentration limits of the biomass shared metabolites and/or the relative differences in the uptake efficiencies of community members. In addition, this analysis revealed that addition of a new member to an existing community can significantly affect the behavior and composition of the community exemplified in this study by the dominance of tri-culture by *S. oneidensis* in the long run.

It is worth noting that a community-level objective function for purely competitive interactions is unnecessary and one can revert to simpler and computationally less expensive methods such as the DMMM procedure.[12] As such, OptCom and d-

OptCom procedures are suitable for modeling microbial communities with at least one cooperative (positive) interaction among the community members. Even though a universal community-level fitness function is not known yet, maximization of the total community biomass concentration (or flux) can be deemed as a reasonable surrogate, when considering the entire community as a unified "super-organism" analogous to a single species. Alternatively, it may be possible to discern a community-level fitness function in some cases by using meta-genomic and meta-transcriptomic data and identifying the dominant set of metabolic functions that are present (i.e., whose genes are highly expressed) under a certain condition. Notably, the objective function of the outer problem in OptCom and d-OptCom can be also used to represent a desired phenotypic behavior of the community thereby providing the opportunity to identify how interspecies metabolic interactions or intracellular flux distributions should be modified in order to satisfy a desired behavior. This was shown in this study by the simulation of uranium reduction capability of the uranium-reducing communities. Taking one step further, OptCom and d-OptCom can be readily adjusted to identify optimal "community engineering" strategies, to achieve a desired objective. These engineering strategies could be in the form of manipulating the environment for natural communities where genetic modification of the community members is not viable. For example, d-OptCom can be adjusted to identify optimal patterns of Fe(III), lactate, or acetate additions, or combinations thereof, in order to reduce the actual uranium concentration in the environment below the standard safety threshold.[44] For synthetic microbial communities where the targeted modification of community members is possible, d-OptCom can be adjusted to identify the optimal intervention strategies for the community members leading to, for example, the targeted overproduction of a desired product from otherwise indigestible resources.

ASSOCIATED CONTENT

Supporting Information

Details of the mathematical formulation for d-OptCom and simulation parameters for the case studies. This material is available free of charge via the Internet at http://pubs.acs.org.

AUTHOR INFORMATION

Corresponding Author

*Tel: +1 814 863 9958. Fax: +1 814 865 7846. E-mail: costas@psu.edu.

Author Contributions

[†]A.R.Z. and M.M.I. are joint first authors.

Author Contributions

A.R.Z. and C.D.M. conceived and coordinated the study, participated in its design and helped to draft the manuscript. A.R.Z. and M.M.I. performed the d-OptCom and regular OptCom simulations (and data analysis), respectively, and drafted the manuscript. All authors read and approved the final manuscript.

Notes

The authors declare no competing financial interest.

ACKNOWLEDGMENTS

REFERENCES

(1) Follows, M. J., Dutkiewicz, S., Grant, S., and Chisholm, S. W. (2007) Emergent biogeography of microbial communities in a model ocean. Science 315 (5820), 1843−6.

(2) The Human Microbiome Project Consortium (2012) A framework for human microbiome research. Nature 486 (7402), 215−221.

(3) The Human Microbiome Project Consortium (2012) Structure, function, and diversity of the healthy human microbiome. Nature 486 (7402), 207−214.

(4) Karlsson, F. H., Nookaew, I., Petranovic, D., and Nielsen, J. (2011) Prospects for systems biology and modeling of the gut microbiome. Trends Biotechnol. 29 (6), 251−8.

(5) Walter, J., and Ley, R. (2011) The human gut microbiome: Ecology and recent evolutionary changes. Annu. Rev. Microbiol. 65, 411−29.

(6) Warnecke, F., Luginbuhl, P., Ivanova, N., Ghassemian, M., Richardson, T. H., Stege, J. T., Cayouette, M., McHardy, A. C., Djordjevic, G., Aboushadi, N., Sorek, R., Tringe, S. G., Podar, M., Martin, H. G., Kunin, V., Dalevi, D., Madejska, J., Kirton, E., Platt, D., Szeto, E., Salamov, A., Barry, K., Mikhailova, N., Kyrpides, N. C., Matson, E. G., Ottesen, E. A., Zhang, X., Hernandez, M., Murillo, C., Acosta, L. G., Rigoutsos, I, Tamayo, G., Green, B. D., Chang, C., Rubin, E. M., Mathur, E. J., Robertson, D. E., Hugenholtz, P., and Leadbetter, J. R. (2007) Metagenomic and functional analysis of hindgut microbiota of a wood-feeding higher termite. Nature 450 (7169), 560−565.

(7) Wirth, R., Kovacs, E., Maroti, G., Bagi, Z., Rakhely, G., and Kovacs, K. L. (2012) Characterization of a biogas-producing microbial community by short-read next generation DNA sequencing. Biotechnol. Biofuels 5 (1), 41.

(8) Katsuyama, C., Nakaoka, S., Takeuchi, Y., Tago, K., Hayatsu, M., and Kato, K. (2009) Complementary cooperation between two syntrophic bacteria in pesticide degradation. J. Theor. Biol. 256 (4), 644−54.

(9) Li, X., Li, P., Lin, X., Zhang, C., Li, Q., and Gong, Z. (2008) Biodegradation of aged polycyclic aromatic hydrocarbons (PAHs) by microbial consortia in soil and slurry phases. J. Hazard. Mater. 150 (1), 21−6.

(10) Mbadinga, S. M., Wang, L. Y., Zhou, L., Liu, J. F., Gu, J. D., and Mu, B. Z. (2011) Microbial communities involved in anaerobic degradation of alkanes. Int. Biodeter. Biodegr. 65 (1), 1−13.

(11) Bacosa, H. P., Suto, K., and Inoue, C. (2012) Bacterial community dynamics during the preferential degradation of aromatic hydrocarbons by a microbial consortium. Int. Biodeter. Biodegr. 74, 109−115.

(12) Zhuang, K., Izallalen, M., Mouser, P., Richter, H., Risso, C., Mahadevan, R., and Lovley, D. R. (2011) Genome-scale dynamic modeling of the competition between Rhodoferax and Geobacter in anoxic subsurface environments. ISME J. 5 (2), 305−16.

(13) Mouser, P. J., N'Guessan, A. L., Elifantz, H., Holmes, D. E., Williams, K. H., Wilkins, M. J., Long, P. E., and Lovley, D. R. (2009) Influence of heterogeneous ammonium availability on bacterial community structure and the expression of nitrogen fixation and ammonium transporter genes during in situ bioremediation of uranium-contaminated groundwater. Environ. Sci. Technol. 43 (12), 4386−92.

(14) Van Nostrand, J. D., Wu, L., Wu, W. M., Huang, Z., Gentry, T. J., Deng, Y., Carley, J., Carroll, S., He, Z., Gu, B., Luo, J., Criddle, C. S., Watson, D. B., Jardine, P. M., Marsh, T. L., Tiedje, J. M., Hazen, T. C., and Zhou, J. (2011) Dynamics of microbial community composition and function during in situ bioremediation of a uranium-contaminated aquifer. Appl. Environ. Microbiol. 77 (11), 3860−3869.

(15) Ueda, S., and Earle, R. L. (1972) Microflora of activated-sludge. J. Gen. Appl. Microbiol. 18 (3), 239−&.

(16) Wagner, M., and Loy, A. (2002) Bacterial community composition and function in sewage treatment systems. Curr. Opin. Biotechnol. 13 (3), 218−27.

(17) Sabra, W., Dietz, D., Tjahjasari, D., and Zeng, A. P. (2010) Biosystems analysis and engineering of microbial consortia for industrial biotechnology. *Eng. Life Sci. 10* (5), 407−421.

(18) Shrestha, U. T. *Microbial Association-Microbial Interaction.* 2009; http://upendrats.blogspot.com/2009/08/microbial-association-microbial.html (accessed Nov. 2013).

(19) Hansen, S. K., Rainey, P. B., Haagensen, J. A. J., and Molin, S. (2007) Evolution of species interactions in a biofilm community. *Nature 445* (7127), 533−536.

(20) Xavier, J. B. (2011) Social interaction in synthetic and natural microbial communities. *Mol. Syst. Biol. 7*, 483.

(21) Fuhrman, J. A. (2009) Microbial community structure and its functional implications. *Nature 459* (7244), 193−199.

(22) Wintermute, E. H., and Silver, P. A. (2010) Emergent cooperation in microbial metabolism. *Mol. Syst. Biol. 6*, 407.

(23) Minty, J. J., Singer, M. E., Scholz, S. A., Bae, C. H., Ahn, J. H., Foster, C. E., Liao, J. C., and Lin, X. N. (2013) Design and characterization of synthetic fungal-bacterial consortia for direct production of isobutanol from cellulosic biomass. *Proc. Natl. Acad. Sci. U.S.A. 110* (36), 14592−7.

(24) Wintermute, E. H., and Silver, P. A. (2010) Dynamics in the mixed microbial concourse. *Genes Dev. 24* (23), 2603−14.

(25) Finn, R. K., and Wilson, R. E. (1954) Fermentation process control—Population dynamics of a continuous propagator for microorganisms. *J. Agric. Food Chem. 2* (2), 66−69.

(26) Tu, B. P., Kudlicki, A., Rowicka, M., and McKnight, S. L. (2005) Logic of the yeast metabolic cycle: Temporal compartmentalization of cellular processes. *Science 310* (5751), 1152−8.

(27) Stolyar, S., Van Dien, S., Hillesland, K. L., Pinel, N., Lie, T. J., Leigh, J. A., and Stahl, D. A. (2007) Metabolic modeling of a mutualistic microbial community. *Mol. Syst. Biol. 3*, 92.

(28) Bizukojc, M., Dietz, D., Sun, J., and Zeng, A. P. (2010) Metabolic modelling of syntrophic-like growth of a 1,3-propanediol producer, *Clostridium butyricum*, and a methanogenic archeon, *Methanosarcina mazei*, under anaerobic conditions. *Bioprocess Biosyst. Eng. 33* (4), 507−23.

(29) Lewis, N. E., Schramm, G., Bordbar, A., Schellenberger, J., Andersen, M. P., Cheng, J. K., Patel, N., Yee, A., Lewis, R. A., Eils, R., Konig, R., and Palsson, B. O. (2010) Large-scale in silico modeling of metabolic interactions between cell types in the human brain. *Nat. Biotechnol. 28* (12), 1279−85.

(30) Tzamali, E., Poirazi, P., Tollis, I. G., and Reczko, M. (2009) Computational identification of bacterial communities. *World Acad. Sci. Eng. Technol. 52*, 269.

(31) Nagarajan, H., Embree, M., Rotaru, A. E., Shrestha, P. M., Feist, A. M., Palsson, B. O., Lovley, D. R., and Zengler, K. (2013) Characterization and modelling of interspecies electron transfer mechanisms and microbial community dynamics of a syntrophic association. *Nat. Commun. 4*, 2809.

(32) Ibarra, R. U., Fu, P., Palsson, B. O., DiTonno, J. R., and Edwards, J. S. (2003) Quantitative analysis of *Escherichia coli* metabolic phenotypes within the context of phenotypic phase planes. *J. Mol. Microbiol. Biotechnol. 6* (2), 101−8.

(33) Tzamali, E., Poirazi, P., Tollis, I. G., and Reczko, M. (2011) A computational exploration of bacterial metabolic diversity identifying metabolic interactions and growth-efficient strain communities. *BMC Syst. Biol. 5*, 167.

(34) Segre, D., Vitkup, D., and Church, G. M. (2002) Analysis of optimality in natural and perturbed metabolic networks. *Proc. Natl. Acad. Sci. U.S.A. 99* (23), 15112−7.

(35) Borenstein, E., and Feldman, M. W. (2009) Topological signatures of species interactions in metabolic networks. *J. Comput. Biol. 16* (2), 191−200.

(36) Freilich, S., Kreimer, A., Borenstein, E., Yosef, N., Sharan, R., Gophna, U., and Ruppin, E. (2009) Metabolic-network-driven analysis of bacterial ecological strategies. *Genome Biol. 10* (6), R61.

(37) Lehmann, L., and Keller, L. (2006) The evolution of cooperation and altruism—A general framework and a classification of models. *J. Evol. Biol. 19* (5), 1365−76.

(38) Nadell, C. D., Foster, K. R., and Xavier, J. B. (2010) Emergence of spatial structure in cell groups and the evolution of cooperation. *PLoS Comput. Biol. 6* (3), e1000716.

(39) Shou, W., Ram, S., and Vilar, J. M. (2007) Synthetic cooperation in engineered yeast populations. *Proc. Natl. Acad. Sci. U.S.A. 104* (6), 1877−82.

(40) Vallino, J. J. (2003) Modeling microbial consortiums as distributed metabolic networks. *Biol. Bull. 204* (2), 174−9.

(41) Frey, E. (2010) Evolutionary game theory: Theoretical concepts and applications to microbial communities. *Phys. A 389* (20), 4265−4298.

(42) Mahadevan, R., Edwards, J. S., and Doyle, F. J., 3rd (2002) Dynamic flux balance analysis of diauxic growth. *Biophys. J. 83* (3), 1331−40.

(43) Song, H.-S., DeVilbiss, F., and Ramkrishna, D. (2013) Modeling metabolic systems: The need for dynamics. *Curr. Opin. Chem. Eng. 2*, 373.

(44) Zhuang, K., Ma, E., Lovley, D. R., and Mahadevan, R. (2012) The design of long-term effective uranium bioremediation strategy using a community metabolic model. *Biotechnol. Bioeng. 109* (10), 2475−83.

(45) Salimi, F., Zhuang, K., and Mahadevan, R. (2010) Genome-scale metabolic modeling of a clostridial co-culture for consolidated bioprocessing. *Biotechnol. J. 5* (7), 726−38.

(46) Hanly, T. J., and Henson, M. A. (2011) Dynamic flux balance modeling of microbial co-cultures for efficient batch fermentation of glucose and xylose mixtures. *Biotechnol. Bioeng. 108* (2), 376−85.

(47) Hanly, T. J., and Henson, M. A. (2013) Dynamic metabolic modeling of a microaerobic yeast co-culture: Predicting and optimizing ethanol production from glucose/xylose mixtures. *Biotechnol. Biofuels 6* (1), 44.

(48) Zomorrodi, A. R., and Maranas, C. D. (2012) OptCom: A multi-level optimization framework for the metabolic modeling and analysis of microbial communities. *PLoS Comput. Biol. 8* (2), e1002363.

(49) Sahinidis, N. V. (1996) BARON: A general purpose global optimization software package. *J, Global Optim, 8* (2), 201−205.

(50) Feist, A. M., Henry, C. S., Reed, J. L., Krummenacker, M., Joyce, A. R., Karp, P. D., Broadbelt, L. J., Hatzimanikatis, V., and Palsson, B. O. (2007) A genome-scale metabolic reconstruction for *Escherichia coli* K-12 MG1655 that accounts for 1260 ORFs and thermodynamic information. *Mol. Syst. Biol. 3*, 121.

(51) Lovley, D. R., Holmes, D. E., and Nevin, K. P. (2004) Dissimilatory Fe(III) and Mn(IV) reduction. *Adv. Microb. Physiol. 49*, 219−86.

(52) Wall, J. D., and Krumholz, L. R. (2006) Uranium reduction. *Annu. Rev. Microbiol. 60*, 149−66.

(53) Anderson, R. T., Vrionis, H. A., Ortiz-Bernad, I., Resch, C. T., Long, P. E., Dayvault, R., Karp, K., Marutzky, S., Metzler, D. R., Peacock, A., White, D. C., Lowe, M., and Lovley, D. R. (2003) Stimulating the *in situ* activity of Geobacter species to remove uranium from the groundwater of a uranium-contaminated aquifer. *Appl. Environ. Microbiol. 69* (10), 5884−91.

(54) Vrionis, H. A., Anderson, R. T., Ortiz-Bernad, I., O'Neill, K. R., Resch, C. T., Peacock, A. D., Dayvault, R., White, D. C., Long, P. E., and Lovley, D. R. (2005) Microbiological and geochemical heterogeneity in an *in situ* uranium bioremediation field site. *Appl. Environ. Microbiol. 71* (10), 6308−18.

(55) Cotter, J. L., Chinn, M. S., and Grunden, A. M. (2009) Ethanol and acetate production by *Clostridium ljungdahlii* and *Clostridium autoethanogenum* using resting cells. *Bioprocess Biosyst. Eng. 32* (3), 369−80.

(56) Sun, J., Sayyar, B., Butler, J. E., Pharkya, P., Fahland, T. R., Famili, I., Schilling, C. H., Lovley, D. R., and Mahadevan, R. (2009) Genome-scale constraint-based modeling of *Geobacter metallireducens*. *BMC Syst. Biol. 3*, 15.

(57) Mahadevan, R., Bond, D. R., Butler, J. E., Esteve-Nunez, A., Coppi, M. V., Palsson, B. O., Schilling, C. H., and Lovley, D. R. (2006) Characterization of metabolism in the Fe(III)-reducing organism

Geobacter sulfurreducens by constraint-based modeling. *Appl. Environ. Microbiol.* 72 (2), 1558−68.

(58) Risso, C., Sun, J., Zhuang, K., Mahadevan, R., DeBoy, R., Ismail, W., Shrivastava, S., Huot, H., Kothari, S., Daugherty, S., Bui, O., Schilling, C. H., Lovley, D. R., and Methe, B. A. (2009) Genome-scale comparison and constraint-based metabolic reconstruction of the facultative anaerobic Fe(III)-reducer *Rhodoferax ferrireducens*. *BMC Genomics* 10, 447.

(59) Pinchuk, G. E., Hill, E. A., Geydebrekht, O. V., De Ingeniis, J., Zhang, X., Osterman, A., Scott, J. H., Reed, S. B., Romine, M. F., Konopka, A. E., Beliaev, A. S., Fredrickson, J. K., and Reed, J. L. (2010) Constraint-based model of *Shewanella oneidensis* MR-1 metabolism: A tool for data analysis and hypothesis generation. *PLoS Comput. Biol.* 6 (6), e1000822.

(60) Pinchuk, G. E., Geydebrekht, O. V., Hill, E. A., Reed, J. L., Konopka, A. E., Beliaev, A. S., and Fredrickson, J. K. (2011) Pyruvate and lactate metabolism by *Shewanella oneidensis* MR-1 under fermentation, oxygen limitation, and fumarate respiration conditions. *Appl. Environ. Microbiol.* 77 (23), 8234−40.

(61) Tang, Y. J., Meadows, A. L., Kirby, J., and Keasling, J. D. (2007) Anaerobic central metabolic pathways in *Shewanella oneidensis* MR-1 reinterpreted in the light of isotopic metabolite labeling. *J. Bacteriol.* 189 (3), 894−901.

(62) Tang, Y. J., Meadows, A. L., and Keasling, J. D. (2007) A kinetic model describing *Shewanella oneidensis* MR-1 growth, substrate consumption, and product secretion. *Biotechnol. Bioeng.* 96 (1), 125−33.

(63) Ulrich, K., Veeramani, H., Schofield, E. J., Sharp, J. O., Suvorova, E. T., Stubbs, J. E., Lezama-Pacheco, J. S., Barrows, C. J., Cerrato, J. M., Campbell, K. M., Yabusaki, S. B., Long, P. L., Bernier-Latmani, R., Giammar, D. E., and Bargar, J. R. Biostimulated uranium immobilization within aquifers: From bench scale to field experiments. In *Mine Water—Managing the Challenges*, Rüde, R. T., Freund, A., and Wolkersdorfer, C., Eds.; IMWA, Aachen, Germany, 2011; pp 627−631.

(64) Yabusaki, S. B., Fang, Y., Waichler, S. R., and Long, P. E. (2010) *Processes, Properties, and Conditions Controlling In Situ Bioremediation of Uranium in Shallow, Alluvial Aquifers*, U.S. Nuclear Regulatory Commission, Office of Nuclear Regulatory Research, Richland, WA.

(65) Bencheikh-Latmani, R., Williams, S. M., Haucke, L., Criddle, C. S., Wu, L., Zhou, J., and Tebo, B. M. (2005) Global transcriptional profiling of *Shewanella oneidensis* MR-1 during Cr(VI) and U(VI) reduction. *Appl. Environ. Microbiol.* 71 (11), 7453−60.

(66) Yabusaki, S. B., and U.S. Nuclear Regulatory Commission. Office of Nuclear Regulatory Research. (2010) *Processes, Properties, and Conditions Controlling In Situ Bioremediation of Uranium in Shallow, Alluvial Aquifers*, U.S. Nuclear Regulatory Commission, Office of Nuclear Regulatory Research, Washington, DC, p 1 online resource (111 p.) col. ill. http://purl.fdlp.gov/GPO/gpo6097.

(67) Zhao, J., Fang, Y., Scheibe, T. D., Lovley, D. R., and Mahadevan, R. (2010) Modeling and sensitivity analysis of electron capacitance for *Geobacter* in sedimentary environments. *J. Contamin. Hydrol.* 112 (1−4), 30−44.

(68) Zhao, J., Scheibe, T. D., and Mahadevan, R. (2011) Model-based analysis of the role of biological, hydrological and geochemical factors affecting uranium bioremediation. *Biotechnol. Bioeng.* 108 (7), 1537−48.

(69) YA, G., and DR, L. (1992) Enzymatic uranium precipitation. *Environ. Sci. Technol.* 26, 205−207.

(70) Cologgi, D. L., Lampa-Pastirk, S., Speers, A. M., Kelly, S. D., and Reguera, G. (2011) Extracellular reduction of uranium via *Geobacter* conductive pili as a protective cellular mechanism. *Proc. Natl. Acad. Sci. U.S.A.* 108 (37), 15248−52.

(71) Sanford, R. A., Wu, Q., Sung, Y., Thomas, S. H., Amos, B. K., Prince, E. K., and Loffler, F. E. (2007) Hexavalent uranium supports growth of *Anaeromyxobacter dehalogenans* and *Geobacter* spp. with lower than predicted biomass yields. *Environ. Microbiol.* 9 (11), 2885−93.